Identifying the Most Effective Data Processing for Fatigue Delamination Growth in FRPs Insights on Artificial Data Simulation

Monticeli, Francisco Maciel; Mosleh, Yasmine; Pascoe, John-Alan

Publication date
2024

Document Version
Final published version

Published in
Proceedings of the 21st European Conference on Composite Materials

Citation (APA)
Monticeli, F. M., Mosleh, Y., & Pascoe, J.-A. (2024). Identifying the Most Effective Data Processing for Fatigue Delamination Growth in FRPs: Insights on Artificial Data Simulation. In C. Binetruy, & F. Jacquemin (Eds.), *Proceedings of the 21st European Conference on Composite Materials: Volume 8 - Special Sessions* (Vol. 8, pp. 571-578). The European Society for Composite Materials (ESCM) and the Ecole Centrale de Nantes..

Identifying the Most Effective Data Processing for Fatigue Delamination Growth in FRPs: Insights on Artificial Data Simulation

Francisco Maciel Monticeli[1*], Yasmine Mosleh[2], John-Alan Pascoe[1]

[1] Faculty of Aerospace Engineering, Aerospace Structures & Materials Department, Delft University of Technology, Kluyverweg 1, 2629 HS Delft, The Netherlands
Email: F.M.Monticeli@tudelft.nl, J.A.Pascoe@tudelft.nl
[2] Faculty of Civil Engineering and Geosciences, Department of Engineering Structures, Delft University of Technology, Stevinweg 1, 2628 CN Delft, The Netherlands
Email: Y.Mosleh@tudelft.nl
[*] Corresponding author: Monticeli, FM (F.M.Monticeli@tudelft.nl)

Keywords: Carbon fibre-reinforced polymer, fatigue delamination, artificial neural network, synthetic data, data processing.

Abstract
This paper investigates the fatigue-induced delamination growth in carbon fibre-reinforced polymer (CFRP), considering different fibre orientation combinations. The study explores the application of Artificial Neural Networks (ANN) in the simulation of fatigue delamination behaviour to reduce the number of experimental tests required for fatigue evaluation and eventual certification. The research aims to evaluate the effectiveness of ANN at different stages of data processing, including raw data simulation and final curve estimation. The results show that applying ANN at the raw data stage provides flexibility in modelling, with error < 10%. In addition, when ANN is applied directly to the final Paris curve, it minimises errors and increases reliability, allowing for a more cost-effective fatigue evaluation process. The study highlights the importance of the data processing stages in determining the accuracy of fatigue delamination predictions with AI modelling, thus informing strategies for efficient fatigue evaluation of CFRP components in structural applications.

1. Introduction

Carbon Fibre Reinforced Polymer (CFRP) is widely used in structural components due to its ability to reduce weight while maintaining the high stiffness required for the application. One of the main limitations of applying CFRP is the low delamination strength, as interlaminar fracture is dominated by cohesive and adhesive failure, which is significantly weaker than fibre fracture [1]. In addition, CFRP poses a significant challenge in terms of certification for structural applications, as the modification of lay-up and fibre orientation can lead to entirely different mechanical behaviours and consequently increase the number of tests required in the qualification pyramid for materials and structures [2,3]. Van der Panne et al. [4] showed that the different fibre orientations at the delamination interface under cyclic loading change the failure mechanisms, modifying the formation of fibre bridging and the saturation of the Paris curve. This confirms the need to extend the coupon tests for each lay-up used. However, this could lead to a significant increase in certification costs and could make structural projects using CFRP infeasible.

The current approach to certifying composite materials for primary aircraft structures under European Safety Agency (EASA) and Federal Aviation Authority (FAA) regulations is based on analysis-assisted certification, which provides the standards for allowable-based certification [5]. Several methods have been applied, such as numerical/computational methods based on finite element analysis [6], statistical-based analysis (e.g., Taguchi, surface response method, among others) [7] and artificial intelligence (AI), aiming to minimise certification costs by reducing the number of coupon tests. Zhang et al. [8] applied an artificial neural network (ANN) to the FE model to predict mixed-mode delamination under

different loading ratios, using the AI method as an intermediate subroutine of the numerical simulation to reduce the number of coupon experiments. On the other hand, Loban et al. [9] applied artificial modelling directly to experimental raw data of residual damage according to several input parameters, allowing the prediction of several combinations of levels that are not experimentally accessible by analytical models.

Allegri [10] demonstrated the application of single hidden layer neural networks to model the Paris curves in modes I, II, and mixed-mode with several stress ratios. The results show a level of accuracy equal to those obtained using the Hartman-Schijve equation (variation of the Paris model). This work demonstrates that using artificial intelligence to simulate data is a viable solution to provide interactive analysis of multiple input parameters inaccessible to analytical models. It can also reduce the number of coupon-level experiments required to validate and certify components on a larger scale. However, artificial data estimation could be applied to several stages of data analysis/processing, from the reproduction of raw data acquisition to the final processed data.

Intending to reduce the number of experiments at coupon level, this work initially proposes training an ANN to model fatigue delamination and access crack propagation behaviour in fibre orientation combinations not accessed experimentally. However, some questions remain regarding the application of artificial intelligence methods to data generation: what is the influence of ANN application in the specific data analysis stage? Would it be possible to determine the contribution of artificial data generated at each data processing stage? To answer the above questions, this work aims to determine the most effective stage of data processing for simulating artificial data and to understand how artificial data affects the accuracy of data processing. The main contribution is to evaluate the accuracy of artificial data from fatigue crack propagation curves using an ANN to model unexplored curves with different fibre orientations, regarding the most effective stage of data processing. The ANN was trained on experimental results from mode I fatigue delamination over three fibre orientations at the delamination interface: (0//0), (0//45) and (0//90). Three stages of data processing are proposed for artificial data estimation:

i) Raw data (compliance and crack length per cycle) – captured directly from experimental tests.
ii) Post-processing (*G-N* and *a-N* curves) – after application of ASTM D5528 [11] procedures.
iii) Final processed data, Paris curves (da/dN *vs* G_{max}) – after application of ASTM D5528 [11] and D6115 [12] procedures.

The error generated for each analysis was compared and experimentally validated by predicting the fatigue crack propagation curve for the laminate with a new interface (0//15).

2. Methodology

2.1. Materials and mechanical test procedures

Double cantilever beam (DCB) specimens were manufactured from IM7/8552 unidirectional carbon fibre/epoxy prepreg from Hexcel®. The prepreg was laid up into different plates with the following stacking sequence $[0_{11}/(\mathbf{0}//\boldsymbol{\theta})/0_{11}]$, where the θ is at the delamination mid-plane and represents 0, 45, and 90º for ANN training and 15º for the validation. A 13 µm PTFE insert film with a length of 50 mm was added in the laminate mid-plane. The laminates were hand-laid with 24 layers and cured in the autoclave at 110 ºC for 60 min and then 180ºC for 120 min, with a vacuum of 0.2 bar and 7 bar of pressure. Specimens were prepared with dimensions of 160 × 25 × 3 mm^3, following ASTM D5528 [11]. The ply elastic properties are: longitudinal and transverse Young's modulus (E_1 = 164 GPa, E_2 = 12 GPa), ply shear modulus (G_{12} = 5 GPa), and major Poisson's ratio (ν_{12} = 0.362) [13].

Fatigue delamination was performed under displacement control following ASTM D6115 [12]. The maximum displacement was set to 90% of the critical displacement (δ_C). The tests were performed at a frequency of 2.5 Hz with a displacement ratio ($R = \delta_{min}/\delta_{max}$) = 0.1, using an MTS hydraulic fatigue

testing machine equipped with a 500 N load cell. During the tests, images of the laminate surface were taken to measure crack propagation at 100-cycle intervals. The modified compliance calibration (MCC) method was used to measure the strain energy (Eq. 1), and the Paris law similitude parameter used was G_{max} (Eq. 2).

$$G_{IC} = \frac{3P_c^2(C/N_1)^{2/3}}{2A_1 bh} \cdot F \tag{1}$$

$$\frac{da}{dN} = \alpha(G_{max})^{\beta} \tag{2}$$

where, G_{IC} is the fracture toughness, P_c is the critical load, C is the compliance, N_1 large displacement and loading block correction factor (≈ 1), F is large displacement correction factor (≈ 1), A_1 is the slope of the plot of a/h versus $(C/N_1)^{1/3}$, b is the width, h id the thickness, da/dN is the crack propagation rate, G_{max} is the similitude parameter for the strain energy release rate (SERR), α and β are the fitting constants.

2.2. ANN method

Before the ANN, a Python subroutine was performed to input the relative elastic properties (E_x, E_y, G_{xy}, v_{xy}) based on the ply elastic properties and lay-up: number of plies and fibre orientation. At the same time, the same Python subroutine was used to determine the D_c and B_t values, which represent the ratio of plane stress to plane strain flexural stiffness (Eq. 3) and the amount of bend/twist coupling in the laminate (Eq. 4), respectively. The ANN plug-in in MatLab was used to train, validate and test the proposed neural networks; 70% of the data sets were used for training, while the rest were used for validation and testing. One-layer and two-layer neural networks were optimised for performance using the trial-and-error approach. The best-performing ANN was the single hidden network with 20 nodes and a normalised mean squared error (MSE) < 10^{-2}, with the number of epochs varying according to the procedure. Figure 1 illustrates the ANN scheme where the input parameters were the relative elastic properties, coupling coefficients, specimen dimensions, fracture toughness, fracture toughness at the saturated fibre bridging zone and fibre orientation at the interface. The responses were the raw data (compliance curve versus crack length/thickness), the first processed data (G-N and a-N curves) and the Paris curve (da/dN versus G_{max}). The hyperbolic tangent activation functions allow the modelling of non-linear relationships within the experimental data. The weighting algorithm used was elastic backpropagation with backtracking, while the error function used was MSE minimisation.

$$D_c = \frac{D_{12}^2}{D_{11}D_{22}} \tag{3}$$

$$B_t = \left|\frac{D_{16}}{D_{11}}\right| \tag{4}$$

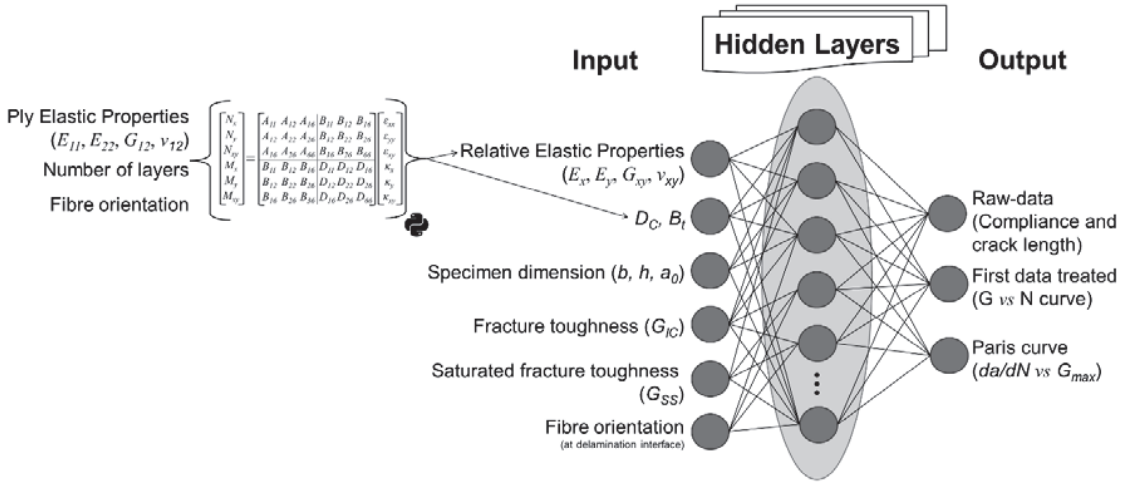

Figure 1. Scheme of input/output in ANN modelling.

Figure 2 shows the flowchart of the data analysis. The data from (0//0), (0//45) and (0//90) were used for training, and then the data from laminate (0//15) were simulated to validate the modelling. The ANN application follows three paths according to the objectives of this work: *i)* simulation of raw data, and then the apply MCC methods and the power law equation to the simulated data; *ii)* after the raw data, the MCC method was applied and then the ANN were carried out to simulate *G-N* and *a-N* curves (after the first data analysis), followed by the application of the power law equation to provide the Paris curve; finally, the third path *iii)* where the ANN where applied to directly simulate the Paris curve (*da/dN versus* G_{max}). This series of tests aims to analyse the error generated by the simulated data at the different stages of data processing (Fig. 2) and compare the final Paris curve estimated for the laminate (0//15). In the end, it will be possible to compare the best stage for generating artificial data and evaluate the ANN application effect at each stage.

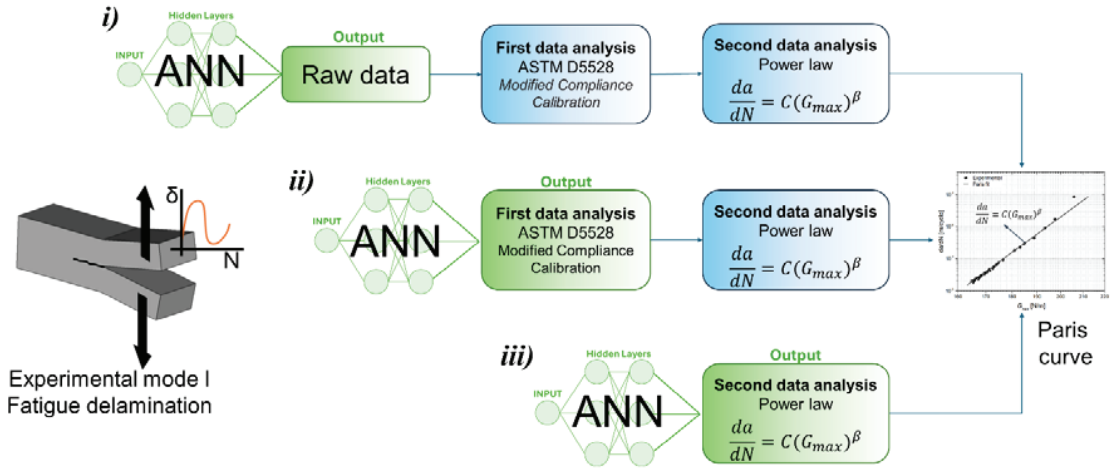

Figure 2. Flowchart of data analysis using ANN to produce data at: *i)* raw data simulation, *ii)* first data analysis simulation and *iii)* Paris curve simulation.

3. Results and discussion

Figure 3 shows the experimental results of modelling the fatigue delamination curves for laminates with the interface (0//0), (0//45), and (0//90) for both the experimental and predicted curves for the validation.

The points on each curve represent the experimental values, and the lines represent ANN fitting. Figure 3a shows the results of path (*i*), where the ANN method was applied to raw data. The advantage of using the ANN for raw data is the freedom to post-process the data without dependence on the SERR equation, compliance method, the similitude parameter (*G*) and the *da/dN* data reduction method. The dependence on the ANN-raw data is related to the geometry and lay-up parameters [$f(b,h,a_0,\theta)$] since the force and displacement results directly relate to the crack growth in this stage. As a first result (Fig. 3a), the ANN model showed an error of less than 3.58%, which was associated with an appropriate curve fit.

Figures 3b and 3c show the second modelling path (*ii*), where the ANN method was applied after the first data processing, i.e., after using the MCC SEER equation. The advantage of this stage is the independence of the geometric parameters (*b* and *h*) since the SEER aspects are already considered a function of the bending stress of the beam. Also, it is independent of the similitude parameters (*G*) and the *da/dN* data reduction method. On the other hand, all modelling from this stage forward is a dependent function of the MCC equation [*f(MMC)*]. In other words, if another standard equation or *J-integral* were applied, the dispersion between the models could be associated with an error in the ANN modelling. The error generated for this second case was 3.45%, similar to those found previously, considering that each model was optimised by training on experimental data.

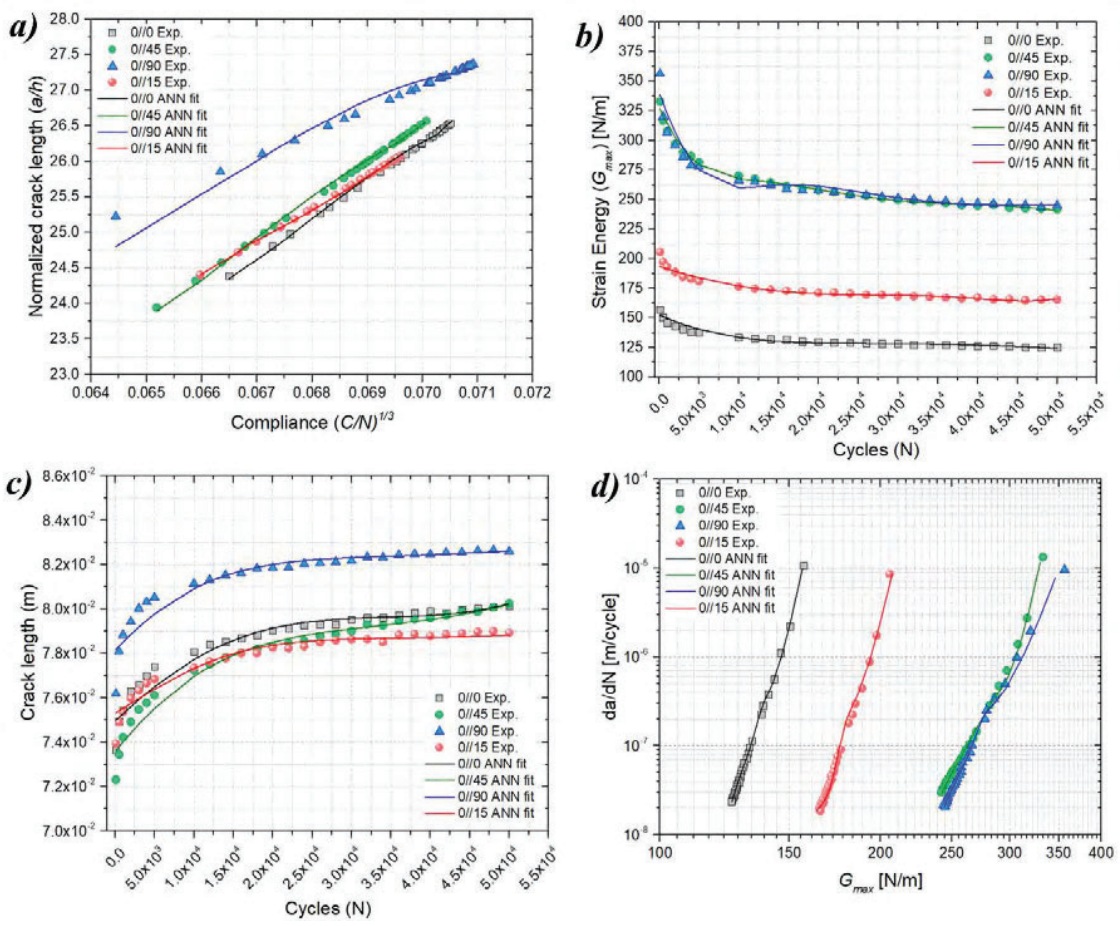

Figure 3. ANN simulation data for: a) raw data (*i*), b) *G-N* curve (*ii*), c) *a-N* curve (*ii*) and d) Paris curve (*iii*).

Figure 3d shows the third ANN application path (*iii*), where the neural network was applied to directly generate the final curve of *da/dN* versus G_{max}. Note that the dots are the experimental results, and the lines represent the AI-predicted data. In other words, the Paris Power Law has yet to be applied to these curves. Applying ANN at this stage can provide faster modelling of the most important curve for crack propagation analysis (the Paris curve) without adding a post-process subroutine for new calculations and data analysis. On the other hand, the artificial results depend on the equation and compliance method used, the *da/dN* curve reduction method and the similitude parameter used [*f(MCC, da/dN, G)*]. The error generated at this modelling stage was 3.46%.

The error was similar for all stages, suggesting an initial independence from the stage of ANN application to generate artificial data. Although there are some limitations regarding dependence on the standard functions when simulating data, new training could easily be performed from the original model to generate the new desired curve. For example, when using different equations to obtain the SEER values (e.g., *J-integral*), a new ANN training could be performed to avoid the intrinsic dispersion generated between the models. Considering that the neural network applied at each stage provides the Paris curves, Figure 4 shows the experimental and simulated results to give the Paris model. Experimental results of the curve for the laminate with the interface (0//15) are represented by black dots. The red dots are the results of the raw data simulated by ANN and then applied to Eq. 1 (MCC), using G_{max} as a similitude parameter and power law to reduce the *a-N* curve. The blue dots are the results when the ANN is used to generate second stage data (*G-N* and *a-N*), and then G_{max} is used as a similitude parameter with a power law to reduce the *a-N* curve. Finally, the green dots are the curves generated when the ANN directly simulates the Paris curve. For each data set (experimental and predicted), the power law from the Paris model was applied in the linear region to capture the constants α and β. The error generated according to the ANN application in each stage was captured (Table 1).

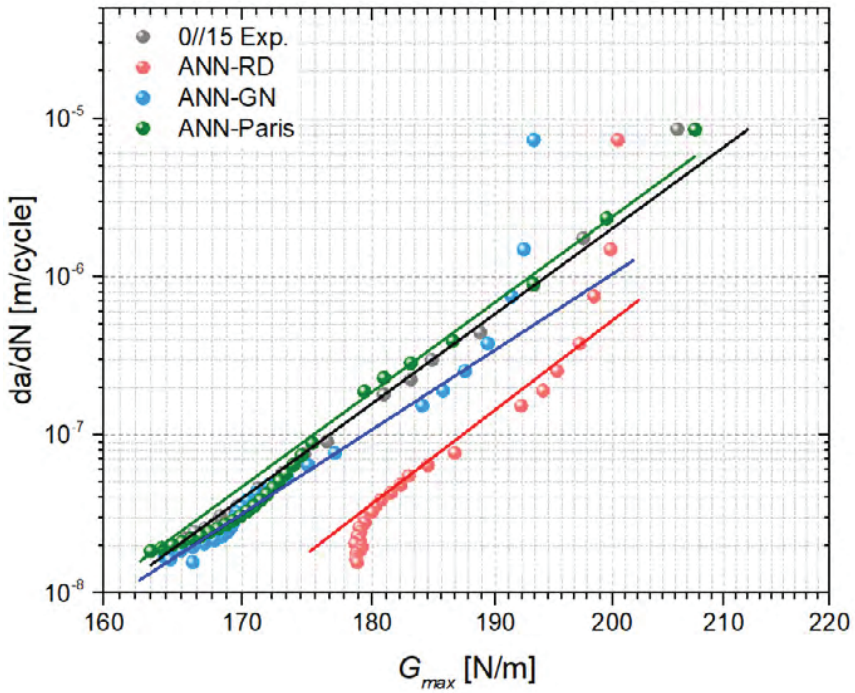

Figure 4. Paris curve comparative curve for (0//15) simulated and experimental data.

The curve generated when the ANN is applied in the first step (*i* – raw data) is the one that visually represents the most significant shift in the curve and changes in the threshold range of SEER from the experimental values. The errors for the angle coefficient (β) were 0.81% but presented a shift in alpha

values of 91%. The errors between the start and end of the curve were 2.58 and 8.04%, respectively. The mean squared error of the curve was 10.41 N/m. This increase in the error generated from raw data to the final Paris curve is a consequence of the accumulated error generated in each parameter P, A_1 and C from the MCC equation (Eq. 1) and the new data reduction of the *da/dN* curve.

The Paris model resulting from the application of ANN in the second stage (*ii* – *G-N*, *a-N*) presented an angular coefficient error (β) of 11.05% and, although it is in the same range of G_{max}, the constant α presented a high significant value because of change in the curve slope, which is associated to a shift in *da/dN* data reduction behaviour. In addition, the error between the beginning ($G_{max,b}$) and the end ($G_{max,u}$) of the G_{max} values was 6.10% and 0.52%, respectively, giving a mean square error (MSE) of the curve of 2.83 N/m. In the second step, the accumulated error from the P, A_1 and C parameters of Eq. 1 was removed (as they are taken from the experiments and not simulated).

Table 1. Error analysis between ANN modelling for different stages of data processing.

Variable	Exp. data	Raw data ANN	*error* (%)	*G-N / a-N* ANN	*error* (%)	Paris ANN	*error* (%)
α (m/cycle)	1×10^{-62}	9×10^{-64}	*91.00*	1×10^{-56}	*>> 100*	5×10^{-65}	*99.50*
β	24.43	24.63	*0.81*	21.737	*11.05*	24.49	*0.23*
$^{a}G_{max,i}$	205.76	200.45	*2.58*	193.20	*6.10*	207.35	*0.77*
$^{b}G_{max,u}$	165.49	178.79	*8.04*	166.35	*0.52*	163.33	*1.30*

a – Initial (*i*) value of *Gmax* in the Paris curve, b – ultimate (*u*) value of *Gmax* in the Paris curve at 50 k cycles.

The curve using simulation in the final stage of data processing (*iii*) showed a significant reduction in error. Although the constant α remained with an error close to 100%, the angular coefficient β error was 0.23 %. The errors at the beginning and end of the G_{max} range were 0.77 and 1.30 %, respectively, and the mean square error of the curve was 1.20 N/m. Although this model is directly dependent on the SEER equations, compliance parameters and *da/dN* data reduction used in the previous stages of data processing, it represents a significant reduction in the errors in data simulated artificially, thus ensuring higher precision in the results obtained.

Given the reduced dependence on SEER, compliance calibration, similitude parameter and *da/dN* data reduction, applying ANN at the raw data stage provides greater freedom in the modelling of data processing. However, when the standardised models are applied to the estimate curves from the initial simulated data, the accumulation of error in the forward equation significantly increases the dispersion. This indicates that the number of errors found could increase with more data processing steps. Therefore, the ANN application stage directly affects the Paris model error. The direct application to generate the final curve presents greater match with the experimental results and higher reliability.

4. Conclusions

In this study, fatigue-induced delamination growth was investigated at interfaces (0//0), (0//45), and (0//90) to train, validate, and test the proposed neural networks and (0//15) was used to validate the simulation method. ANN was a feasible method for predicting crack propagation curves and simulating configurations not explored experimentally, with an error of less than 3.5% for each data processing stage.

Applying ANN to raw data provides greater freedom in post-processing modelling, with a Paris curve error < 10% and an MSE error of 10.41 N/m. On the other hand, applying ANN directly to the final stage Paris curve significantly minimises the error (< 2%) and MSE, generating a more direct application to the target curve for fatigue delamination. In conclusion, the ANN application directly into the Paris curve enables the reduction of the coupon test level, thus reducing the cost associated with fatigue evaluation. In addition, the data processing stage directly affects the accuracy of the Paris curve.

Acknowledgments
Funded by the European Union under GA No. 101091409. Views and opinions expressed are however those of the author(s) only and do not necessarily reflect those of the European Union. Neither the European Union nor the granting authority can be held responsible for them.

References
[1] R. Khan, R. Alderliesten, R. Benedictus. Two-parameter model for delamination growth under mode i fatigue loading (Part B: Model development). *Compos Part A Appl Sci Manuf*, (65): 201–10, 2014. https://doi.org/10.1016/j.compositesa.2014.06.008.
[2] M. Pogosyan, E. Nazarov, A. Bolshikh, V. Koroliskii, N. Turbin, K. Shramko. Aircraft composite structures integrated approach: A review. *J Phys Conf Ser*, (1925): 1–16, 2021. https://doi.org/10.1088/1742-6596/1925/1/012005.
[3] A.J. Brunner, R. Alderliesten, J. Pascoe. In-Service Delaminations in FRP Structures under Operational Loading Conditions: Are Current Fracture Testing and Analysis on Coupons Sufficient for Capturing the Essential Effects for Reliable Predictions? *Materials (Basel)* (16): 1–24, 2023.
[4] M. van der Panne, J.A. Pascoe. Fatigue delamination growth - Is UD testing enough? *Procedia Struct Integr*, (42): 449–56, 2022.
[5] R. Whitehead, R. Deo. A building block approach to design verification testing of primary composite structure. *Proc 24th AIAA/ASME/ASCE/AHS SDM Conf*, v1: 473–7, 1983. https://doi.org/10.2514/6.1983-947.
[6] F. Starace, S.D. Orlando, M. Guida, F. Marulo. Experimental study of a virtual allowables approach for the design of composite aircraft structures. *Proc Inst Mech Eng Part C J Mech Eng Sci*, (235): 2529–41, 2021. https://doi.org/10.1177/0954406220987862.
[7] Y. Zhang, X. Xu. Predicting the delamination factor in carbon fibre reinforced plastic composites during drilling through the Gaussian process regression. *J Compos Mater*, (55): 2061–8, 2021. https://doi.org/10.1177/0021998320984245.
[8] B. Zhang, G. Allegri, S.R. Hallett. Embedding artificial neural networks into twin cohesive zone models for composites fatigue delamination prediction under various stress ratios and mode mixities. *Int J Solids Struct*, (236-237): 111311, 2022. https://doi.org/10.1016/j.ijsolstr.2021.111311.
[9] O. Laban, S. Gowid, E. Mahdi, F. Musharavati. Experimental investigation and artificial intelligence-based modeling of the residual impact damage effect on the crashworthiness of braided Carbon/Kevlar tubes. *Compos Struct*, (243): 112247, 2020. https://doi.org/10.1016/j.compstruct.2020.112247.
[10] G. Allegri. Modelling fatigue delamination growth in fibre-reinforced composites : Power-law equations or artificial neural networks ? *Mater Des*, (155): 59–70, 2018. https://doi.org/10.1016/j.matdes.2018.05.049.
[11] ASTM D5528. Standard Test Method for Mode I Interlaminar Fracture Toughness of Unidirectional Fiber-Reinforced Polymer Matrix Composites. *Am Soc Test Mater* (1): 1–14, 2021. https://doi.org/10.1520/D5528_D5528M-21.
[12] ASTM D6115. Standard Test Method for Mode I Fatigue Delamination Growth Onset of Unidirectional Fiber-Reinforced Polymer Matrix Composites. *Am Soc Test Mater*, (1): 1–7, 2021. https://doi.org/10.1520/D6115-97R19.
[13] Hexply®. HexPly 8552 Product Data. *Hexcel Composites Publication FTA 072e*, (1): 1-6, 2013.